Heliyon

ELSEVIER

Received:
3 October 2018
Revised:
24 December 2018
Accepted:
31 January 2019

Cite as:
S. Madan Kumar. 3D energy frameworks of dimethylbenzophenone tetramorphs.
Heliyon 5 (2019) e01209.
doi: 10.1016/j.heliyon.2019.e01209

3D energy frameworks of dimethylbenzophenone tetramorphs

S. Madan Kumar*

DST-PURSE Lab, Mangalore University, India

* Corresponding author.

E-mail addresses: madan.mx@gmail.com, madanmx@mangaloreuniversity.ac.in (S. Madan Kumar).

Abstract

The tetramorph[th] crystals of 4,4−dimethylbenzophenone (**D**) were obtained using slow-evaporation crystallization method and the structure is elucidated using single crystal X-ray diffraction technique. **D** crystallizes in the orthorhombic crystal system (space group *Pbca*) with cell parameters $a = 14.6986\ (11)$ Å, $b = 6.1323\ (4)$ Å, $c = 26.2730\ (18)$ Å, $V = 2368.2\ (3)$ Å^3 and $Z = 8$. In the crystal structure, intermolecular interaction of the type C—H$^{\cdots}\pi$ stabilizes the crystal packing. This polymorph is the fourth candidate of its kind and second candidate in the orthorhombic crystal system. The structural comparisons and crystal packing of tetramorphs (**A**, **B**, **C** and **D**) are analyzed using molecular structures, Hirshfeld surfaces, enrichment ratios (*E*) and energy frameworks. The conformational differences are observed in all the tetramorphs and the intercontacts H···H and C···H contributes around 85 % to the Hirshfeld surfaces. The *E* ratio provides evidence of H···H, C···H and O···H intercontacts having high propensity to form contacts in the crystal packing. The average energy (dimer formation) for each polymorph is calculated from energy framework analysis. The systematic comparison of crystal packing in tetramorphs through 3D-topology is visualized. In the energy-frameworks of the crystal packing, dispersion energy dominates over the electrostatic energy. Overall, the molecular packings of the four polymorphic structures are different.

Keyword: Condensed matter physics

https://doi.org/10.1016/j.heliyon.2019.e01209

1. Introduction

A polymorphic phenomenon in the solid state system is one of the hot topics in the crystallographic community. In this phenomenon, the same compound appears in different crystal structures (at least two) [1]. The review report on polymorphism systematic screening of history and facts revealed molecular crystal polymorphs are frequent [2]. There are differences in the three dimensional (3D) similarities among polymorphs [3]. The concept of supramolecular synthon [4] and supramolecular constructs are used to analyse spatial arrangements of intermolecular interactions in crystals (molecular packing) and to identify the similarity among crystal structures and polymorphs, (packing similarities) respectively [5]. Further, packing polymorphism deals with conformational rigid molecule packing in different arrangements, while the conformational polymorphism deals with flexible molecule rearranging to produce more than one different conformation in the solid state [6]. They show different physical properties and other physico-chemical properties according to the polymorph [7]. One of the organic moieties 'benzophenone' shows prevalent polymorphism and among them 4,4−dimethylbenzophenone has three polymorphic structures [8]. The reported trimorphs of the title molecule crystallize in the crystal systems trigonal (**A**: CSD refcode FEVMUO0; space group − $P_3 21$) [8], orthorhombic (**B**: CSD refcode FEVMUO01; space group − $P2_12_12_1$) [9], and monoclinic (**C**: CSD refcode FEVMUO02; space group − $P2_1/c$) [10].

Benzophenones are biologically active compounds [11, 12] and are used as UV-filters in sunscreens [13]. The Enrichment ratio (E) is used identify the propensity of the pair of elements (X, Y) to form contacts in the crystals [14, 15]. The energy framework concept [16, 17, 18] is a computational graphical tool for representing the magnitudes of interaction energies within the crystal packing. 3D topology of the intermolecular interactions relates to the properties of the molecular crystals. In this paper, I present the crystallization, single crystal X-ray diffraction, Hirshfeld surfaces computational method, enrichment ratios and 3D energy frameworks of the tetramorph of 4,4−dimethylbenzophenone (Figs. 1 and 3). In addition, the reported trimorphs **A**, **B** and **C** were analyzed and compared using Hirshfeld surfaces, enrichment ratios and 3D energy frameworks.

2. Methodology

2.1. Materials and crystallization

4,4−dimethylbenzophenone (**D**) (Sigma-Aldrich) with molecular grade were used for the crystallization experiments. About 50 grams of **D** is dissolved in binary solvents of DMF and Ethanol at ambient conditions. The slow evaporation resulted in colourless crystals after few days.

https://doi.org/10.1016/j.heliyon.2019.e01209

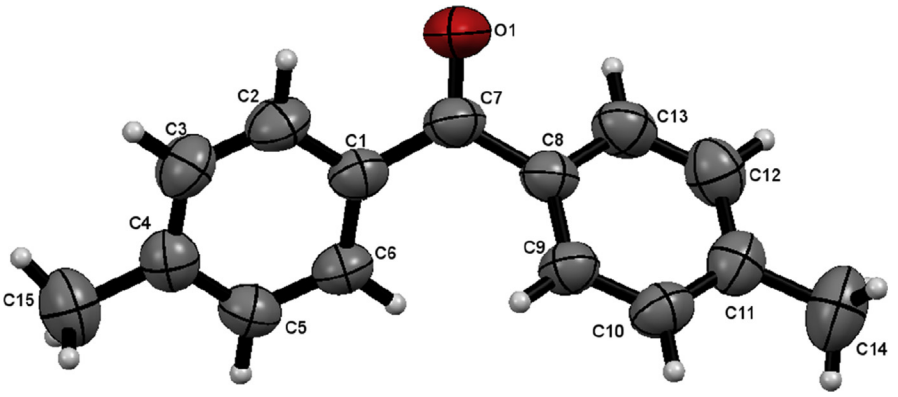

Fig. 1. ORTEP view with atom labelling system of the title compound with displacement ellipsoids are drawn at the 50% probability level.

2.2. Single crystal X-ray diffraction

The diffracted X-ray intensity data for single crystal of compound **D** were collected at a temperature of 296 K on a Rigaku Saturn724 diffractometer using graphite monochromated radiation (Mo-Kα). The diffracted intensities obtained after the experiments were processed using *CrystalClear* [19]. Reflection file after processing is used to solve the structure by direct methods and refined by full-matrix least squares method on F^2 using *SHELXS* and *SHELXL* programs [20] embedded within the Olex2 software [21]. In the first difference Fourier map, non-hydrogen atoms were identified followed by isotropic and anisotropic refinement. The riding model was applied to position hydrogen atoms geometrically and refinement. Final model refinement (ten cycles) difference Fourier map showed no chemical significance peaks. The molecular structure [ORTEP (Fig. 1)] and packing diagrams [Fig. 2] were generated using the software *MERCURY* [22]. Crystal structure and data refinement parameters/values are given in Table 1.

2.3. Hirshfeld surfaces analysis and enrichment ratio (*E*)

The final refined crystallographic information file (CIF) is given as input to the CrystalExplorer 3.1 software [23] to analyze and visualize Hirshfeld Surfaces [24] and their relative 2D fingerprint plots [25]. The parameters d_{norm} (normalized contact distance) and 2D fingerprint plots were used for quantifying/visualizing and decoding of the intercontact in the crystal packing. The dark-red spots on the *dnorm* surface arise as a result of the short interatomic contacts, while the other intermolecular interactions appear as light-red spots. The parameters used on 2D fingerprint plots (Fig. 4: d_i (inside) and d_e (outside) represents the distances to the Hirshfeld surface from the nuclei, with respect to the relative van der Waals radii [*vdW*]. The proportional contribution of intercontact over the surface is visualized by the colour gradient (blue to red) in the fingerprint plots. The Hartree-Fock theory with STO-3G basis set was used to generate electrostatic potential on the Hirshfeld surfaces

https://doi.org/10.1016/j.heliyon.2019.e01209

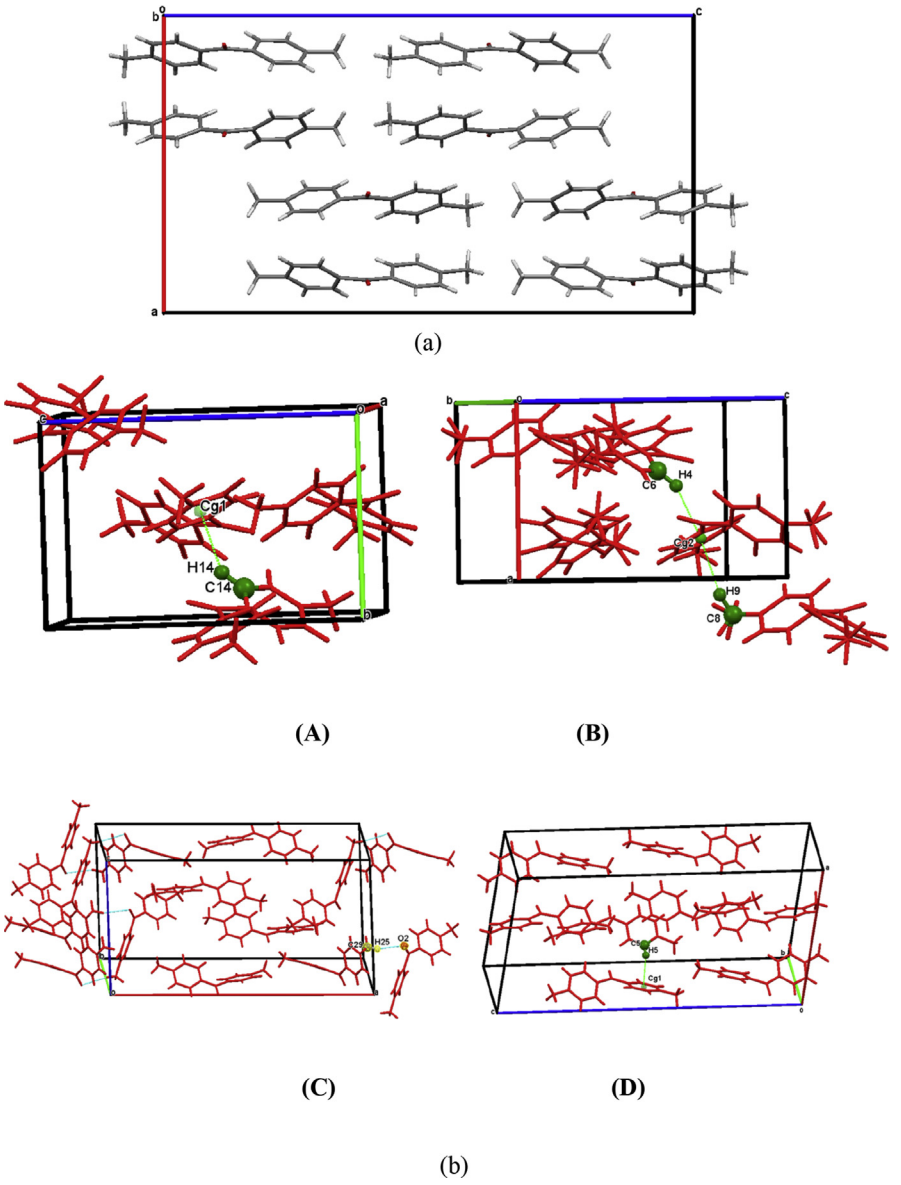

Fig. 2. (**a**) Packing of the compound; a view along b − axis. (**b**) Intermolecular interactions of the tetramorphs (**A**, **B**, **C** and **D**). Atom labels of polymorphs **A**, **B** and **C** kept without changing from the reported article [8].

(Fig. 4). The electrostatic potential surfaces with red region indicates negative electrostatic potential (hydrogen acceptors) and blue region indicates a positive electrostatic potential (hydrogen donor) [26].

The values of intercontacts calculated over Hirshfeld surfaces are used to evaluate the propensities of the pair of elements (X, Y) to form contacts in the crystal and are analyzed using enrichment ratio (E) [14] (Table 4). E is the ratio between the

https://doi.org/10.1016/j.heliyon.2019.e01209

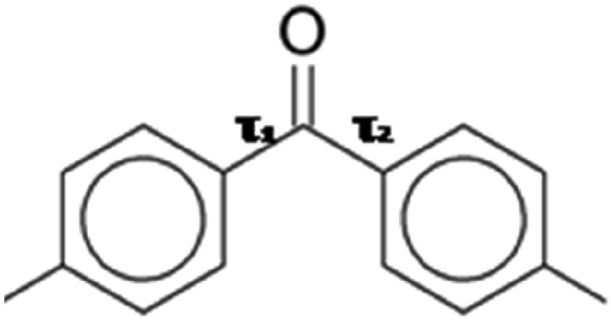

Fig. 3. Chemical diagram of 4,4−dimethylbenzophenone [8].

actual contacts (proportion) in the crystal and random contacts (theoretical proportion). The pairs of element will have high propensity to form contacts and pairs avoid contacts with each other in the crystals if $E > 1$ and $E < 1$, respectively [17, 18].

Table 1. Crystal Data and Structure Refinement details for **D**.

	D
CCDC number	1538365
Empirical formula	C15 H14 O
Formula weight	210.26
Temperature (K)	293 (2)
Wavelength (Kα,Å)	0.71075
Crystal system, space group	orthorhombic, *Pbca*
Unit cell dimensions (Å, °)	$a = 14.6986$ (11) $b = 6.1323$ (4) $c = 26.2730$ (18)
Volume Å^3	2368.2 (3)
Z, Calculated density (Mg/m^3)	8, 1.179
Absorption coefficient (mm^{-1})	0.072
$F_{(000)}$	896
Crystal size mm	0.21 × 0.23 × 0.24
Theta range for data collection (^{0})	2.8 to 26.4
Limiting indices	$-18 \leq h \leq 18$, $-7 \leq k \leq 6$, $-32 \leq l \leq 32$
Reflections collected/unique [R (int)]	24455/2418 [0.091]
Refinement method	Full-matrix least-squares on F^2
Data/restraints/parameters	1586/0/147
R value	0.0726
Goodness-of-fit on F^2	1.04
Largest diff. peak and hole (e. Å^{-3})	0.18 and −0.19

https://doi.org/10.1016/j.heliyon.2019.e01209

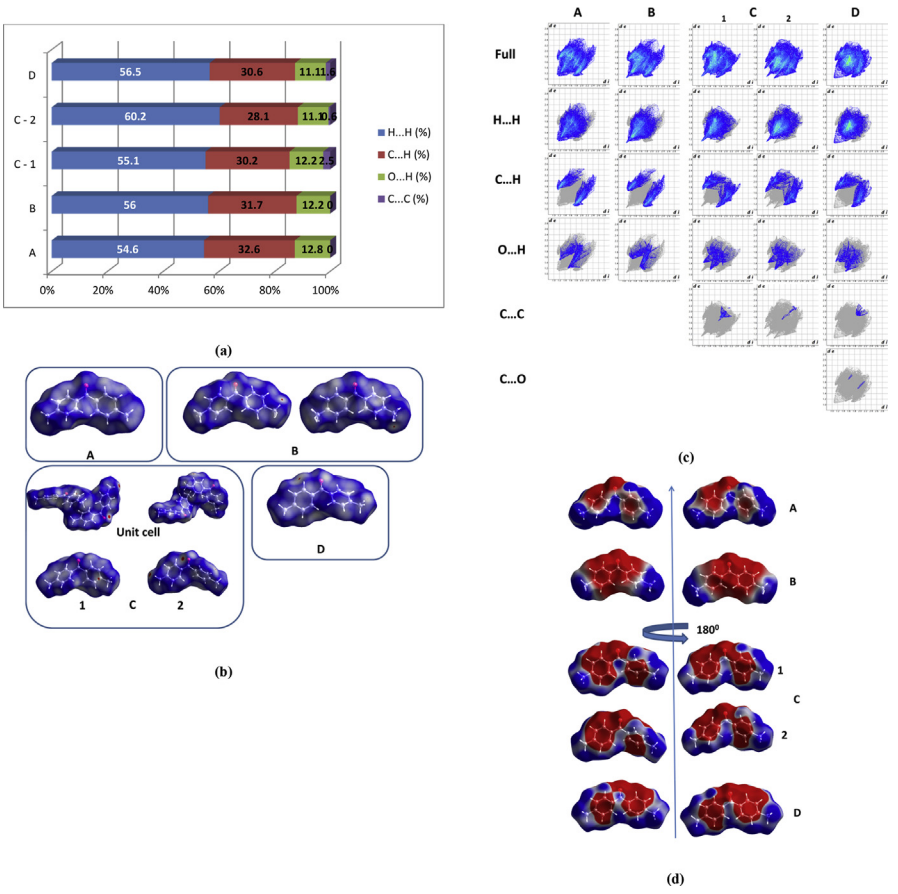

Fig. 4. (a) Percentage contributions of various close intermolecular contacts to the Hirshfeld surface area in tetramorphs (A,B, C-1/C-2 and D) and rotated over 180°. Hirshfeld surfaces (d_{norm} mapped) of tetramorphs. (b), 2D Fingerprint plots (c) and Electrostatic potential surfaces (d) of the tetramorphs.

2.4. 3D energy framework analysis

New version of CrystalExplorer 17 [27] software (CIF as input) was used to calculate, visualize and analyze the 3D energy framework along with intermolecular interaction energies. The single point molecular wavefunction at B3LYP/6-31G (d,p) level of theory is used to calculate the energy by generating a cluster of radius 3.8 Å around the molecule. The neighbouring molecules in the shell around the central molecule are generated by applying crystallographic symmetry operations [17, 18, 28, 29].

3. Results and discussion

3.1. Molecular and crystal structure

The tetramorphth (**D**) crystals of 4,4−dimethylbenzophenone were obtained using binary solvents of DMF and Ethanol at ambient conditions. The **D** molecules

https://doi.org/10.1016/j.heliyon.2019.e01209

crystallize in the orthorhombic crystal system, (space group *Pbca*) with cell parameters $a = 14.6986\ (11)°$, $b = 6.1323\ (4)°$, $c = 26.2730\ (18)°$, $V = 2368.2\ (3)\ Å^3$ and $Z = 8$ (Fig. 1). The reported trimorphs of the title compound **A**, **B** and **C** [8, 9], crystallized in the tetragonal ($P3_221$), orthorhombic ($P2_12_12_1$) and monoclinic ($P2_1/c$) crystal systems, respectively. The **D** is the second polymorph within the orthorhombic crystal system. The dihedral angles between the phenyl rings is $50.63\ (11)^0$. The torsional angle (Table 2: Fig. 3) measured are -15.8 (3)° (τ_1 - O1/C7/C1/C2) and -33.4 (3)° (τ_2 - O1/C7/C8/C13), showing the τ_2 is two times τ_1. The same trend is observed in molecule 2 of polymorph C with slightly different values. The other polymorphs (**A, B, C (1)**: Table 2) don't show this type of trend in the geometry. The polymorph A has similar torsional angles ($\tau_1 = \tau_2$) when compared to other polymorphs. The conformation of all the polymorphs varies according to the crystal system/space group. In the crystal structure **D** (Fig. 2a, Table 3), the molecule stabilizes with intermolecular interactions of the type C5···H5···Cg1 (C1-C6) (Fig. 2b - **D**). Similarly, the other polymorphic crystal structures (Fig. 2b) are stabilized through intermolecular interactions/hydrogen bonds of the type, C···H···π (**A**), C···H···π (**B**), C···H···π (**B**) and C···H···O (**C**:molecule **2**).

3.2. Hirshfeld surfaces and enrichment ratio

Hirshfeld surfaces computational method was used to visualize (Hirshfeld surfaces) and quantify (Fingerprint plots) the intermolecular contacts in tetramophs crystal

Table 2. Torsion angles of the tetramorphs.

	A	B	C (1/2)	D
τ_1 (°)	28.2 (2)	21.1 (3)	−29.6 (2)/−21.4 (2)	−15.8 (3)
τ_2 (°)	28.2 (2)	32.3 (3)	−42.4 (2)/−42.4 (2)	−33.4 (3)
CSD Refcode/CCDC	FEVMUO [8]	FEVMUO01 [8]	FEVMUO02 [8]	1538365 [This work]

Table 3. Intermolecular interactions parameters of tetramoprhs.

D—H...A/Cg		H...A/Cg (Å)	D....A/Cg (Å)	D—H...A/Cg (°)	Symmetry
A					
C14—H14...Cg1		2.71 (4)	3.620 (4)	143 (3)	-1/2 + X,1/2-Y,-Z
B					
C6—H4...Cg2		2.701 (9)	3.625 (3)	144.4 (8)	-X,1/2 + Y,1/2-Z
C8—H9...Cg2		2.68	3.6971 (13)	156	-1/2 + X,1/2-Y,-Z
C					
C29—H25...O2 (**2**)	0.96	2.58	3.509 (6)	162	-X,1/2 + Y,3/2-Z
D					
C5—H5...Cg1		2.81	3.541 (2)	136	1/2-X,-1/2 + Y,Z

https://doi.org/10.1016/j.heliyon.2019.e01209

packing (Fig. 4) [23, 24, 25]. The red spots (surfaces) over the Hirshfeld surfaces indicate the closer contacts representing the intermolecular interactions based on *vdW* separation. In each polymorph, red surfaces vary according to the strength of the intercontacts. Among all the polymorphs, **A** has the least red surface [Fig. 4b]. The Hirshfeld surfaces are used to generate fingerprint plots (Fig. 4c), which are used to quantify intermolecular contacts through histograms and their similarities/ dissimilarities [25]. The variation of the intermolecular contacts in the crystal environment of tetramorphs: **A, B, C (1, 2)** and **D** are revealed by the fingerprint plots and their corresponding values are compared in Fig. 4a. In all the polymorphs, H···H (A:54.6 %, B:56 %, C-1:55.1 %, C-2:60.2 % and D:56.5 %) and O···H (A:32.6 %, B:31.7 %, C-1:30.2 %, C-2:28.1 % and D-30.6 %) together contributes more than 85 % to the Hirshfeld surface area and overall percentage contribution is almost similar in tetramorphs. Other intercontacts observed are O···H (A: 12.8 %, B: 12.2 %, C-1:12.2 %, C-2:11.10 % and D:11.11 %), C···C (C-1:2.5 %, C-2:0.6 % and D:0.5 %) and C···O (D: 0.2 %). The electrostatic potential drawn over the tetramorphs Hirshfeld surfaces are drawn and shown in Fig. 4d. The systematic comparison reveals the polymorph **B** has more red region (electronegative region) when compared to other polymorphic electrostatic potential surfaces. This difference in the electronegative region arises in **B** due to presence of both the +*syn*-periplanar (τ_1) and +*syn*-clinal (τ_2) conformation.

Further, Enrichment ratio (*E*) is calculated for tetramorphs to analyze the intercontacts having high propensity to form contacts in the crystal packing (Tables 4, 5, 6, 7, and 8) [14]. The *E* values of **A** (C···H = 1.29, O···H = 1.29, H···H = 0.91), **B** (C···H = 1.28, O···H = 1.26, H···H = 0.92), **C** (**1/2**: C···H = 1.31/1.1, O···H = 1.31/1.16, H···H = 0.95/1.0) and **D** (C···H = 1.16, O···H = 1.27 and H···H = 0.94) are tabulated in Table. The *E* values of **A, B, C (1,2)** and **D** shows C···H, O···H and H···H have high propensity of forming contacts within the crystal packing.

3.3. Energy framewoks

The crystal packing in the tetramorphs are constructed through the recent computational method 'energy frameworks' integrated with latest version of CrystalExplorer17 [27]. Initially, the interaction energy between the molecular pairs in all the polymorphic forms are calculated [Tables 9, 10, 11, 12, and 13] and used to generate/construct 3D-topology [Fig. 5] frame of the major interactions in the form of energy frameworks. The comparison of the electrostatic, dispersion and total energy frameworks across tetramorphs (Fig. 6) indicates dissimilarities in energy frameworks. However, the views down *a*- and *c*- axis of **A** is comparable as similar to the views down *a*-axis of **B**. Similarly, the views down *b*- and *c*-axis of **C** (molecule 2) are almost similar to the views down *a*-axis of **D**. The dispersion energy term

https://doi.org/10.1016/j.heliyon.2019.e01209

Table 4. Hirshfeld contact surfaces derived random contact and enrichment ratio for the **A**. The data values obtained from Crystal Explorer are written in italics at the top of the table. The enrichment rations were not computed when the 'random contacts' were lower than 0.9 %, as they are not meaningful (NA – Not Applicable).

	A		
Atoms	H	C	O
H	*54.6*		Contacts (%)
C	*32.6*		
O	*12.8*		
Surface %	77.3	16.3	6.4
H	**59.75**		Random contacts (%)
C	**25.20**	2.66	
O	9.90	2.10	0.41
H	**0.91**		Enrichment
C	**1.29**	0	
O	**1.29**	0	NA

Table 5. Hirshfeld contact surfaces derived random contact and enrichment ratio for the **B**. The data values obtained from Crystal Explorer are written in italics at the top of the table. The enrichment rations were not computed when the 'random contacts' were lower than 0.9 %, as they are not meaningful (NA – Not Applicable).

		B	
Atoms	H	C	O
H	*56*		Contacts (%)
C	*31.7*		
O	*12.2*		
Surface %	77.95	15.85	6.1
H	**60.69**		Random contacts (%)
C	**24.71**	2.51	
O	9.51	1.93	0.37
H	**0.92**		Enrichment
C	**1.28**	0	
O	**1.26**	0	NA

https://doi.org/10.1016/j.heliyon.2019.e01209

Table 6. Hirshfeld contact surfaces derived random contact and enrichment ratio for the **C-1**. The data values obtained from Crystal Explorer are written in italics at the top of the table. The enrichment rations were not computed when the 'random contacts' were lower than 0.9 %, as they are not meaningful (NA – Not Applicable).

		C-1	
Atoms	H	C	O
H	*55.1*		Contacts (%)
C	*30.2*	*2.5*	
O	*12.2*	*0*	*0*
Surface %	76.3	17.6	6.1
H	**58.22**		Random contacts (%)
C	**26.86**	3.10	
O	9.31	2.14	0.37
H	**0.95**		Enrichment
C	**1.31**	0.81	
O	**1.31**	0	NA

Table 7. Hirshfeld contact surfaces derived random contact and enrichment ratio for the **C-2**. The data values obtained from Crystal Explorer are written in italics at the top of the table. The enrichment rations were not computed when the 'random contacts' were lower than 0.9 %, as they are not meaningful (NA – Not Applicable).

		C-2	
Atoms	H	C	O
H	*60.2*		Contacts (%)
C	*28.1*	*0.6*	
O	*11.1*	*0*	*0*
Surface %	77.95	16.45	6.1
H	**60.69**		Random contacts (%)
C	**25.65**	2.70	
O	9.51	2.00	0.37
H	**1.00**		Enrichment
C	**1.10**	0.22	
O	**1.16**	0	NA

https://doi.org/10.1016/j.heliyon.2019.e01209

Table 8. Hirshfeld contact surfaces derived random contact and enrichment ratio for the **D**. The data values obtained from Crystal Explorer are written in italics at the top of the table. The enrichment rations were not computed when the 'random contacts' were lower than 0.9 %, as they are not meaningful (NA – Not Applicable).

		D	
Atoms	H	C	O
H	*56.5*		Contacts (%)
C	*30.6*	*1.6*	
O	*11.1*	*0.2*	*0*
Surface %	77.35	17	5.65
H	**59.83**		Random contacts (%)
C	**26.30**	2.89	
O	8.74	1.92	0.32
H	**0.94**		Enrichment
C	**1.16**	0.55	*NA*
O	**1.27**	0.10	NA

Table 9. Molecular pairs and the interaction energies (kJ/mole) obtained from energy framework calculation for **A**. R is the distance between molecular centroids (mean atomic position) in Å. Total energies, only reported for two benchmarked energy models, are the sum of the four energy components, scaled appropriately (see the scale factor below). Energy model is CE-B3LYP...B3LYP/6-31G (d,p) electron densities with K_ele (1.057), K_pol (0.740), K_disp (0.871) and K_rep (0.618). Refer Fig. 5 for Sl. Nos.

Sl. No	**N**	**Symop**	**R**	**Electron Density**	**E_ele**	**E_pol**	**E_dis**	**E_rep**	**E_tot**
i	2	x+1/2,-y+1/2,-z	7.62	B3LYP/6-31G (d,p)	−9.2	−2.1	−22.7	12.3	−23.3
ii	2	−x,y+1/2,− z+1/2	5.85	B3LYP/6−31G (d,p)	−8.1	−1.1	−39.9	23.4	−29.6
iii	2	x+1/2,-y+1/2,- z	7.87	B3LYP/6-31G (d,p)	−3.4	−0.7	−19.3	9.0	−15.4
iv	2	-x+1/2,-y, z+1/2	7.09	B3LYP/6-31G (d,p)	−4.7	−2.1	−23.1	13.3	18.5
v	2	-x+1/2,-y, z+1/2	10.58	B3LYP/6-31G (d,p)	−1.9	−0.9	−8.8	4.5	−7.7
vi	2	x,y,z	12.16	B3LYP/6-31G (d,p)	−0.0	−0.2	−7.5	3.2	−4.7
vii	2	-x,y+1/2, -z+1/2	10.97	B3LYP/6-31G (d,p)	0.3	−0.1	−3.7	1.1	−2.4

https://doi.org/10.1016/j.heliyon.2019.e01209

Table 10. Molecular pairs and the interaction energies (kJ/mole) obtained from energy framework calculation for **B**. R is the distance between molecular centroids (mean atomic position) in Å. Total energies, only reported for two benchmarked energy models, are the sum of the four energy components, scaled appropriately (see the scale factor below). Energy model is CE-B3LYP...B3LYP/6-31G (d,p) electron densities with K_ele (1.057), K_pol (0.740), K_disp (0.871) and K_rep (0.618). Refer Fig. 5 for Sl. Nos.

Sl. No.	N	Symop	R	Electron Density	E_ele	E_pol	E_dis	E_rep	E_tot
i	2	x+1/2,-y+1/2,-z	10.94	B3LYP/6-31G (d,p)	−4.1	−1.4	−5.5	3.5	−8.0
ii	2	-x,y+1/2,- z+1/2	7.66	B3LYP/6-31G (d,p)	−14.8	−7.6	−24.7	14.3	−33.9
iii	2	x+1/2,-y+1/2,- z	5.81	B3LYP/6-31G (d,p)	−15.7	−5.9	−49.2	41.6	−38.1
iv	2	x,y,z	12.17	B3LYP/6-31G (d,p)	−14.0	−5.8	−15.3	13.6	−24.1
v	2	-x+1/2,-y, z+1/2	7.08	B3LYP/6-31G (d,p)	−12.1	−8.6	−28.0	22.2	−29.8
vi	2	-x,y+1/2,-z+1/2	7.90	B3LYP/6-31G (d,p)	−6.8	−6.1	−23.2	12.6	−24.2
vii	2	-x+1/2,-y, z+1/2	10.60	B3LYP/6-31G (d,p)	−19.4	−6.1	−12.5	6.0	−32.1

is more dominating in all the tetramorphs when compared to electrostatic term (Fig. 6).

The net interaction energies in each of the polymoprhs are derived from the pair-wise interaction energies used to plot energy frameworks. During the calculation, the molecules around the residue (symmetry independent molecule) shell are taken and the

Table 11. Molecular pairs and the interaction energies (kJ/mole) obtained from energy framework calculation for **C-1**. R is the distance between molecular centroids (mean atomic position) in Å. Total energies, only reported for two benchmarked energy models, are the sum of the four energy components, scaled appropriately (see the scale factor below). Energy model is CE-B3LYP...B3LYP/6-31G (d,p) electron densities with K_ele (1.057), K_pol (0.740), K_disp (0.871) and K_rep (0.618). Refer Fig. 5 for Sl. Nos.

Sl. No.	N	Symop	R	Electron Density	E_ele	E_pol	E_dis	E_rep	E_tot
i	1	-	7.53	B3LYP/6-31G (d,p)	−4.6	−0.9	−29.7	16.0	−21.5
ii	2	x,y,z	6.08	B3LYP/6-31G (d,p)	−7.0	−4.3	−25.5	17.2	−22.2
iii	2	-x,y+1/2,-z+1/2	6.89	B3LYP/6-31G (d,p)	−2.9	−1.0	−26.7	13.0	−19.1
iv	1	-x,-y-z	9.74		0.4	−0.3	−5.9	1.9	−3.7
v	1	-	8.51	B3LYP/6-31G (d,p)	−0.5	−0.3	−15.9	7.3	−10.1
vi	1	-	11.86	B3LYP/6-31G (d,p)	−0.1	−0.1	−6.7	3.0	−4.2
vii	1	-x,-y,-z	7.44	B3LYP/6-31G (d,p)	−4.4	−1.4	−32.6	12.2	−26.5
viii	1	-	7.44	B3LYP/6-31G (d,p)	−8.2	−2.1	−20.8	9.5	−22.5
ix	1	-	8.89	B3LYP/6-31G (d,p)	−5.1	−0.8	−23.9	16.0	−16.9
x	1	-	12.72	B3LYP/6-31G (d,p)	−0.1	−0.2	−5.4	2.6	−3.3

https://doi.org/10.1016/j.heliyon.2019.e01209

Table 12. Molecular pairs and the interaction energies (kJ/mole) obtained from energy framework calculation for **C-2**. R is the distance between molecular centroids (mean atomic position) in Å. Total energies, only reported for two benchmarked energy models, are the sum of the four energy components, scaled appropriately (see the scale factor below). Energy model is CE-B3LYP...B3LYP/6-31G (d,p) electron densities with K_ele (1.057), K_pol (0.740), K_disp (0.871) and K_rep (0.618). Refer Fig. 5 for Sl. Nos.

Sl. No.	N	Symop	R	Electron Density	E_ele	E_pol	E_dis	E_rep	E_tot
i	1	-	7.53	B3LYP/6-31G (d,p)	−4.6	−0.9	−29.7	16.0	−21.5
ii	0	x,y,z	6.08	B3LYP/6-31G (d,p)	−7.0	−4.3	−25.5	17.2	−22.2
iii	0	-x,y+1/2,-z+1/2	6.89	B3LYP/6-31G (d,p)	−2.9	−1.0	−26.7	13.0	−19.1
iv	0	-x,-y-z	9.74	B3LYP/6-31G (d,p)	0.4	−0.3	−5.9	1.9	−3.7
v	1	-	8.51	B3LYP/6-31G (d,p)	−0.5	−0.3	−15.9	7.3	−10.1
vi	1	-	11.86	B3LYP/6-31G (d,p)	−0.1	−0.1	−6.7	3.0	−4.2
vii	0	-x,-y,-z	7.44	B3LYP/6-31G (d,p)	−4.4	−1.4	−32.6	12.2	−26.5
viii	1	-	7.44	B3LYP/6-31G (d,p)	−8.2	−2.1	−20.8	9.5	−22.5
ix	1	-	8.89	B3LYP/6-31G (d,p)	−5.1	−0.8	−23.9	16.0	−16.9
x	1	-	12.72	B3LYP/6-31G (d,p)	−0.1	−0.2	−5.4	2.6	−3.3
xi	2	-x,y+1/2,-z+1/2	8.05	B3LYP/6-31G (d,p)	−7.4	−1.7	−19.1	12.5	−18.0
xii	1	-x,-y,-z	11.89	B3LYP/6-31G (d,p)	−0.3	−0.2	−6.9	2.8	−4.7
xiii	1	-x,-y,-z	14.41	B3LYP/6-31G (d,p)	0.2	−0.1	−3.8	1.3	−2.3
xiv	2	x,y,z	6.08	B3LYP/6-31G (d,p)	−1.8	−0.6	−24.8	7.4	−19.4
xv	2	x,-y+1/2,z+1/2	7.82	B3LYP/6-31G (d,p)	−4.2	−1.6	−8.1	3.7	−10.4
xvi	2	x,-y+1/2,z+1/2	9.50	B3LYP/6-31G (d,p)	−3.4	−1.6	−6.0	4.2	−7.4

Table 13. Molecular pairs and the interaction energies (kJ/mole) obtained from energy framework calculation for **D**. R is the distance between molecular centroids (mean atomic position) in Å. Total energies, only reported for two benchmarked energy models, are the sum of the four energy components, scaled appropriately (see the scale factor below). Energy model is CE-B3LYP...B3LYP/6-31G (d,p) electron densities with K_ele (1.057), K_pol (0.740), K_disp (0.871) and K_rep (0.618). Refer Fig. 5 for Sl. Nos.

	N	Symop	R	Electron Density	E_ele	E_pol	E_dis	E_rep	E_tot
i	1	-x, -y, -z	7.53	B3LYP/6-31G (d,p)	−2.6	−0.8	−31.5	11.9	−23.4
ii	2	-x, y+1/2, -z+1/2	8.28	B3LYP/6-31G (d,p)	−4.5	−1.6	−21.7	11.4	−17.7
iii	1	-x, -y, -z	8.42	B3LYP/6-31G (d,p)	−7.0	−1.4	−14.5	11.1	−14.2
iv	2	x,y,z	6.13	B3LYP/6-31G (d,p)	−5.4	−3.8	−23.3	13.0	−20.8
v	2	-x+1/2,y+1/2,z	4.85	B3LYP/6-31G (d,p)	−2.9	−1.4	−41.7	20.7	−27.7
vi	2	x, -y+1/2, z+1/2	14.05	B3LYP/6-31G (d,p)	−0.2	−0.1	−5.3	3.0	−3.0
vii	2	-x+1/2, -y, z+1/2	13.80	B3LYP/6-31G (d,p)	−0.0	−0.1	−2.9	0.9	−2.0
viii	2	x, -y+1/2, z+1/2	13.19	B3LYP/6-31G (d,p)	−0.1	−0.2	−4.5	1.0	−3.5

https://doi.org/10.1016/j.heliyon.2019.e01209

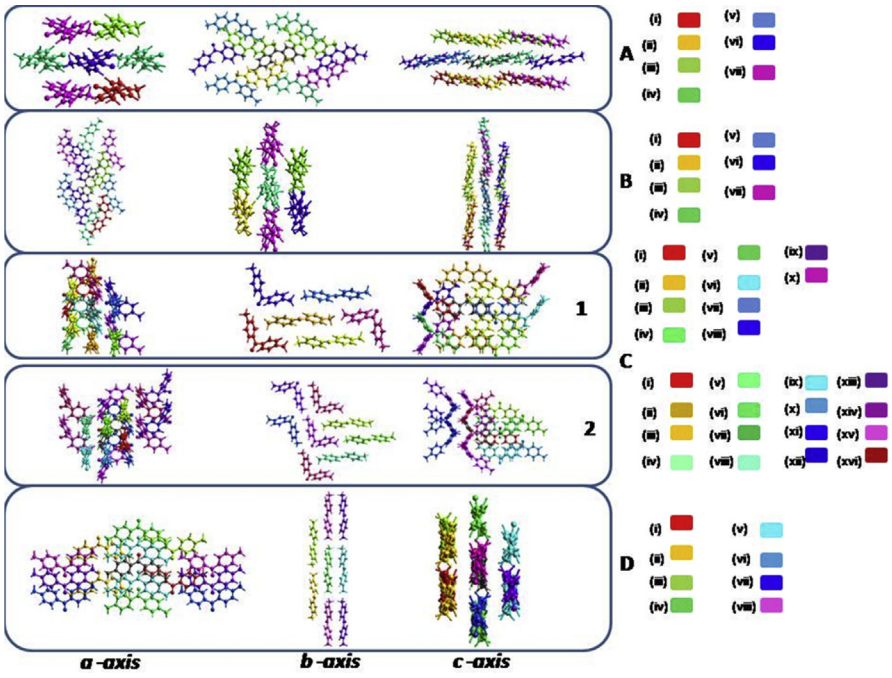

Fig. 5. Color coding of neighbouring molecules with respect to the central molecule (gray) of the tetramorphs (A,B, C-1, C-2 and D). A view along *a*,*b*,*c*-axis. Symmetry molecules around central molecules are represented by respective colours.

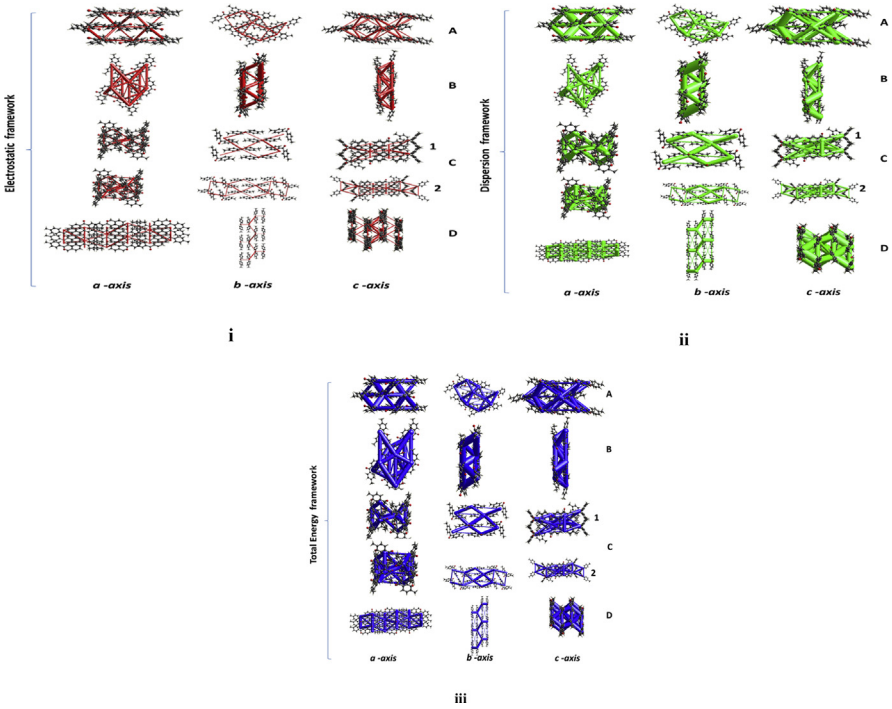

Fig. 6. Energy frameworks corresponding to the different energy components (i. electrostatic, ii. dispersion and iii. total energy framework along a, b and c-axis for tetramorphs A, B, C-1/C-2 and D. The tube size (scale factor) used in all the energy frameworks was 300.

https://doi.org/10.1016/j.heliyon.2019.e01209

Table 14. Interaction Energies of tetramorphs (**A,B, C-1, C-2** and **D**).

	Eele	Epol	Edis	Erepl	Etot	Average Etot (kJ/mole)
A	−27.60	−7.2	−125	66.8	−101.6	−50.8
B	−86.9	−41.5	−158.4	113.8	−190.6	−95.1
C-1	−32.5	−11.4	−193.1	98.7	−150	−75
C-2	−49.4	−17.2	−261.8	130.6	−212.2	−106.1
D	−22.7	−9.4	−145.4	73	−112.3	−56.15

values are listed [Tables 9, 10, 11, 12, and 13]. The overall average net interaction energy with molecules around the chosen radius (shell) is listed in Table 14]. The average total energy (Etot in kJ/mole) for **A, B, C (1/2)** and **D** are -50.8 kJ/mole, -95.1 kJ/mole, -75/-106.1 kJ/mole, and -56.15 kJ/mole, respectively. The Etot of polymorphs **A** and **D** are almost similar. The Etot values of other polymorphs show significant differences.

4. Conclusions

In summary, the tetramorphth crystals of 4,4−dimethylbenzophenone (**D**) were obtained using slow-evaporation crystallization method. This polymorph is the fourth candidate of its kind and second candidate of the orthorhombic crystal system. The structural comparisons and crystal packing of tetramorphs (**A, B, C** and **D**) are analyzed using molecular structures, Hirshfeld surfaces, enrichment ratios (*E*) and energy frameworks. The conformational differences are observed in all the tetramorphs. The *E* values provide evidence of H...H, C...H and O...H intercontacts having high propensity to form contacts in the crystal packing. The energy framework analysis provided average energy between dimers and the 3D-topology of the crystal packing is visualized. Overall, the tetramorphs of the title compound with dissimilarities in molecular packing and packing similarities reveals the scope for more polymorphic candidates and corresponding varying properties.

Declarations

Author contribution statement

S. Madan Kumar: Conceived and designed the experiments; Performed the experiments; Analyzed and interpreted the data; Contributed reagents, materials, analysis tools or data; Wrote the paper.

Funding statement

This research did not receive any specific grant from funding agencies in the public, commercial, or not-for-profit sectors.

https://doi.org/10.1016/j.heliyon.2019.e01209

Competing interest statement

The authors declare no conflict of interest.

Additional information

Data associated with this study has been deposited at Cambridge Crystallographic Data Centre under the accession number CCDC 1538365.

Acknowledgements

Author thank DST-PURSE lab for single crystal X-ray facility.

References

[1] W.C. McCrone, in: D. Fox, M.M. Labes, A. Weissberger (Eds.), Physics and Chemistry of the Organic Solid State 2, Interscience Publishers, New York, USA, 1965, pp. 725−767.

[2] A.J. Cruz-Cabeza, S.M. Reutzel-Edens, J. Bernstein, Facts and fictions about polymorphism, Chem. Soc. Rev. 44 (2015) 8619−8635.

[3] S.J. Coles, T. Threlfall, G. Tizzard, The same but different: isostructural polymorphs and the case of 3-chloromandelic acid, Cryst. Growth Des. 14 (2014) 1623−1628.

[4] G.R. Desiraju, Supramolecular synthons in crystal engineering—a new organic synthesis, Angew. Chem., Int. Ed. Engl. 31 (1995) 2311.

[5] K.K. Jha, S. Dutta, P. Munshi, Isostructural polymorphs: qualitative insights from energy frameworks, CrystEngComm 18 (2016) 8497−8505.

[6] A.Y. Lee, D. Erdemir, A.S. Myerson, Crystal polymorphism in chemical process development, Annu. Rev. Chem. Biomol. Eng. 2 (2011) 259−280.

[7] M.M. Parmar, O. Khan, L. Seton, J.L. Ford, Polymorph selection with morphology control using solvents, Cryst. Growth Des. 7 (2007) 1635−1642.

[8] A.A. Soqaka, C. Esterhuysen, A. Lemmerera, Prevalent polymorphism in benzophenones, Acta Crystallogr. C74 (2018) 465−471.

[9] B. Kojic-Prodic, N. Bresciani-Pahor, D. Horvatic, Structure of 4,4'-dimethylbenzophenone, Acta Crystallogr. C46 (1990) 430−432.

[10] A. Lemmerer, Private Communication (Refcode FEVMUO02), CCDC, Cambridge, England, 2011.

https://doi.org/10.1016/j.heliyon.2019.e01209

[11] S.A. Khanum, B.A. Begum, V. Girish, N.F. Khanum, Synthesis and evaluation of benzophenone-N-ethyl morpholine ethers as anti-inflammatory agents, Int. J. Biomed. Sci. 6 (2010) 60−65.

[12] S.A. Khanum, S. Shashikanth, S. Umesha, R. Kavitha, Synthesis and antimicrobial study of novel heterocyclic compounds from hydroxybenzophenones, Eur. J. Med. Chem. 40 (2005) 1156−1162.

[13] J.C. DINardo, C.A. Downs, Dermatological and environmental toxicological impact of the sunscreen ingredient oxybenzone/benzophenone-3, J. Cosmet. Dermatol. 17 (2017) 15−19.

[14] C. Jelsch, K. Ejsmont, L. Huder, The enrichment ratio of atomic contacts in crystals, an indicator derived from the Hirshfeld surface analysis, IUCrJ 1 (2014) 119−128.

[15] S. Madan Kumar, H. Al-Ostoot Fares, B.C. Manjunath, V.R. Shamprasad, Md. Yasser Hussein Eissa, N. Mahesh, Zabiulla, A.K. Shaukath, N.K. Lokanath, K. Byrappa, Crystal packing analysis of 1-(3,4-dimethoxyphenyl)-3-(4-bromophenyl)prop-2-en-1-one exhibiting a putative halogen bond C—Br···O, J. Mol. Struct. 1156 (2018) 216−223.

[16] M.J. Turner, S.P. Thomas, M.W. Shi, D. Jayatilaka, M.A. Spackman, Energy frameworks: insights into interaction anisotropy and the mechanical properties of molecular crystals, Chem. Commun. 51 (2015) 3735−3738.

[17] S. Madan Kumar, B.N. Lakshminarayana, S. Nagaraju, Sushma, S. Ananda, B.C. Manjunath, N.K. Lokanath, K. Byrappa, 3D energy frameworks of a potential nutraceutical, J. Mol. Struct. 1173 (2018) 300−306.

[18] S. Madan Kumar, Avinash K. Kudva, B.C. Manjunath, P. Naveen, T. Prashanth, Shaukath Ara Khanum, N.K. Lokanath, P. Nagendra, 3D energy framework of a benzophenone acidic dimer, Chem. Data Collect. 19 (2019) 100168.

[19] S.M. Rigaku Crystal Clear, Expert 2.0 R15. Software for Data Collection and Processing, Rigaku Corporation, Tokyo, Japan, 2011.

[20] G.M. Sheldrick, A short history of SHELX, Acta Crystallogr. 64 (2008) 112−122.

[21] O.V. Dolomanov, L.J. Bourhis, R.J. Gildea, J.A.K. Howard, H. Puschmann, OLEX2: a complete structure solution, refinement and analysis program, J. Appl. Crystallogr. 42 (2009) 339−341.

[22] C.F. Macrae, I.J. Bruno, J.A. Chisholm, P.R. Edging-ton, P. McCabe, E. Pidcock, L. Rodriguez-Monge, R. Taylor, J. van de Streek, P.A. Wood,

https://doi.org/10.1016/j.heliyon.2019.e01209

Mercury CSD 2.0 − new features for the visualization and investigation of crystal structures, J. Appl. Crystallogr. 41 (2008) 466−470.

[23] J.J. McKinnon, M.A. Spackman, A.S. Mitchell, Novel tools for visualizing and exploring intermolecular interactions in molecular crystals, J. Acta. Crystallogr. B60 (2004) 627−668.

[24] M.A. Spackman, D. Jayatilaka, Hirshfeld surface analysis, Cryst. Engg. Comm. 11 (2009) 19−32.

[25] M.A. Spackman, J.J. McKinnon, Fingerprinting intermolecular interactions in molecular crystals, CrystEngComm 4 (66) (2002) 378−392.

[26] S. Madan Kumar, B.C. Manjunath, G.S. Lingaraju, M.M.M. Abdoh, M.P. Sadashiva, N.K. Lokanath, A Hirshfeld surface analysis and crystal structure of 2'-[1-(2-Fluoro-Phenyl)-1H-tetrazol-5-Yl]-4-Methoxy-Biphenyl-2-Carbaldehyde, Cryst. Struct. Theor. Appl. 3 (2013) 124−131.

[27] M.J. Turner, J.J. McKinnon, S.K. Wolff, D.J. Grimwood, P.R. Spackman, D. Jayatilaka, M.A. Spackman, CrystalExplorer17, University of Western Australia, 2017.

[28] M.J. Turner, S. Grabowsky, D. Jayatilaka, M.A. Spackman, Accurate and efficient model energies for exploring intermolecular interactions in molecular crystals, J. Phys. Chem. Lett. 5 (2014) 4249−4255.

[29] C.F. Mackenzie, P.R. Spackman, D. Jayatilaka, M.A. Spackman, CrystalExplorer model energies and energy frameworks: extension to metal coordination compounds, organic salts, solvates and open-shell systems, IUCrJ 4 (2017) 575−587.

https://doi.org/10.1016/j.heliyon.2019.e01209